Chapter 2

Mechanical Behavior, Testing, and Manufacturing Properties of Materials

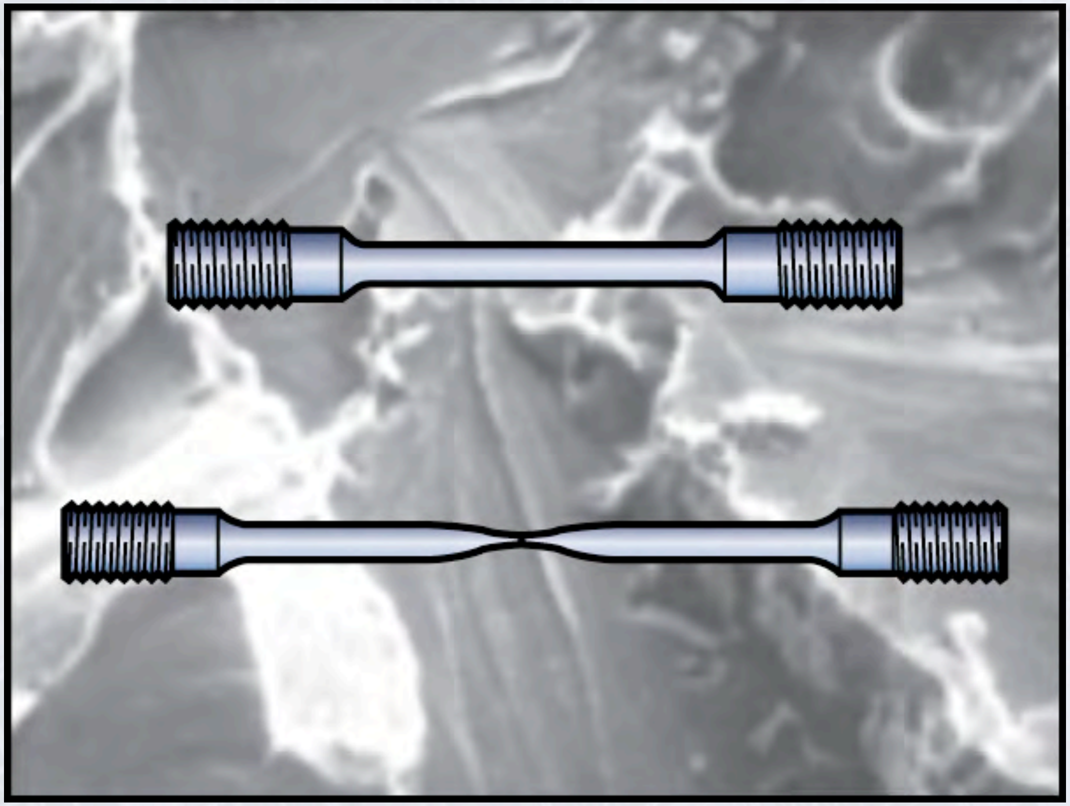

Manufacturing, Engineering & Technology, Fifth Edition, by Serope Kalpakjian and Steven R. Schmid.
ISBN 0-13-148965-8.

Relative Mechanical Properties of Materials

TABLE 2.1

Relative Mechanical Properties of Various Materials at Room Temperature, in Decreasing Order. Metals are in their Alloy Form.

Strength	Hardness	Toughness	Stiffness	Strength/Density
Glass fibers	Diamond	Ductile metals	Diamond	Reinforced plastics
Graphite fibers	Cubic boron nitride	Reinforced plastics	Carbides	Titanium
Kevlar fibers	Carbides	Thermoplastics	Tungsten	Steel
Carbides	Hardened steels	Wood	Steel	Aluminum
Molybdenum	Titanium	Thermosets	Copper	Magnesium
Steels	Cast irons	Ceramics	Titanium	Beryllium
Tantalum	Copper	Glass	Aluminum	Copper
Titanium	Thermosets		Ceramics	Tantalum
Copper	Magnesium		Reinforced plastics	
Reinforced thermosets	Thermoplastics		Wood	
Reinforced thermoplastics	Tin		Thermosets	
Lead	Lead		Thermoplastics	
			Rubbers	

Manufacturing, Engineering & Technology, Fifth Edition, by Serope Kalpakjian and Steven R. Schmid.
ISBN 0-13-148965-8.

Tensile-test Specimen and Machine

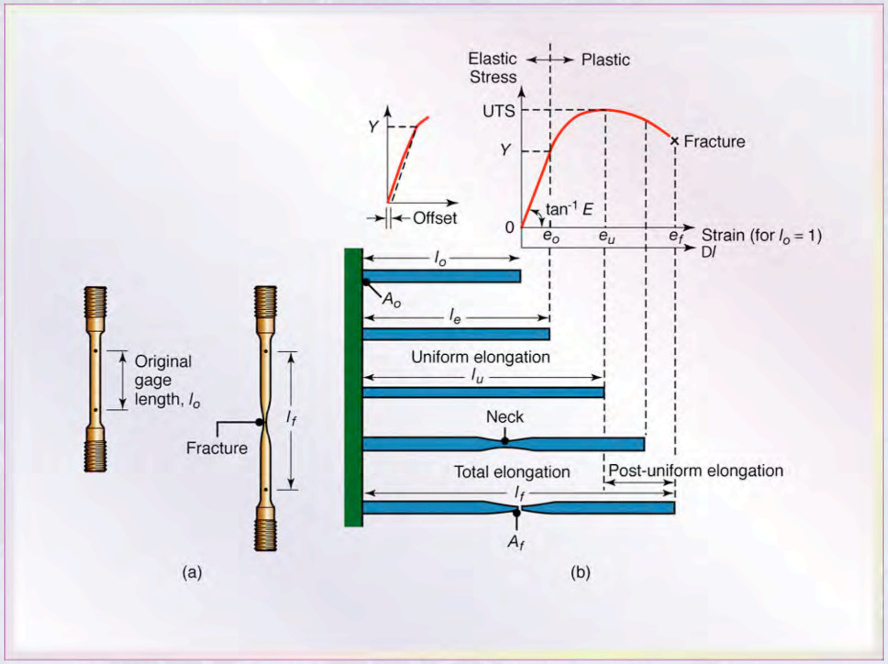

Figure 2.1 (a) A standard tensile-test specimen before and after pulling, showing original and final gage lengths. (b) A tensile-test sequence showing different stages in the elongation of the specimen.

Engineering Stess, $\sigma = \dfrac{P}{A_o}$

Engineering Strain, $e = \dfrac{l - l_o}{l_o}$

Modulus of Elasticity, $E = \dfrac{\sigma}{e}$

True stress, $\sigma = \dfrac{P}{A}$

True strain, $\varepsilon = \ln\left(\dfrac{l}{l_o}\right)$

Manufacturing, Engineering & Technology, Fifth Edition, by Serope Kalpakjian and Steven R. Schmid.
ISBN 0-13-148965-8.

Tension Test Stress-strain Curve

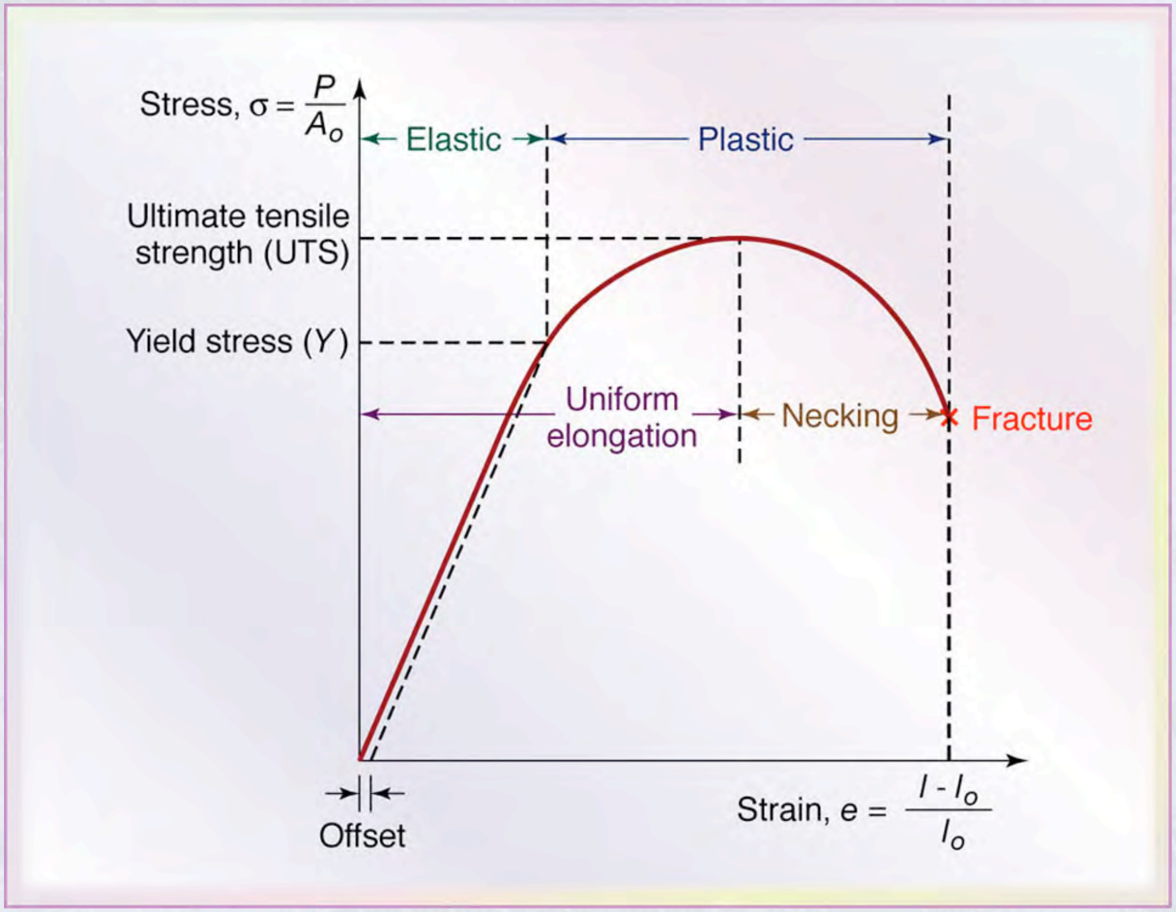

Figure 2.2 A typical stress-strain curve obtained from a tension test, showing various features

Mechanical Properties of Materials

TABLE 2.2

Mechanical Properties of Various Materials at Room Temperature

Metals (Wrought)	*E* (GPa)	*Y* (MPa)	UTS (MPa)	Elongation in 50 mm (%)	Poisson's ratio (ν)
Aluminum and its alloys	69–79	35–550	90–600	45–4	0.31–0.34
Copper and its alloys	105–150	76–1100	140–1310	65–3	0.33–0.35
Lead and its alloys	14	14	20–55	50–9	0.43
Magnesium and its alloys	41–45	130–305	240–380	21–5	0.29–0.35
Molybdenum and its alloys	330–360	80–2070	90–2340	40–30	0.32
Nickel and its alloys	180–214	105–1200	345–1450	60–5	0.31
Steels	190–200	205–1725	415–1750	65–2	0.28–0.33
Titanium and its alloys	80–130	344–1380	415–1450	25–7	0.31–0.34
Tungsten and its alloys	350–400	550–690	620–760	0	0.27
Zinc and its alloys	50	25–180	240–550	65–5	0.27
Nonmetallic Materials					
Ceramics	70–1000	—	140–2600	0	0.2
Diamond	820–1050	—	—	—	—
Glass and porcelain	70–80	—	140	0	0.24
Silicon carbide (SiC)	200–500	—	310–400	—	0.19
Silicon nitride	280–310	—	160–580	—	0.26
Rubbers	0.01–0.1	—	—	—	0.5
Thermoplastics	1.4–3.4	—	7–80	1000–5	0.32–0.40
Thermoplastics, reinforced	2–50	—	20–120	10–1	—
Thermosets	3.5–17	—	35–170	0	0.34
Boron fibers	380	—	3500	0	—
Carbon fibers	275–415	—	2000–3000	0	—
Glass fibers	73–85	—	3500–4600	0	—
Kevlar fibers	62–117	—	2800	0	—
Spectra Fibers	73–100	—	2400–2800	3	—

Note: In the upper table, the lowest values for *E*, *Y*, and UTS and the highest values for elongation are for pure metals. Multiply gigapascals (GPa) by 145,000 to obtain pounds per square in. (psi) and megapascals (MPa) by 145 to obtain psi.

Loading and Unloading of Tensile-test Specimen

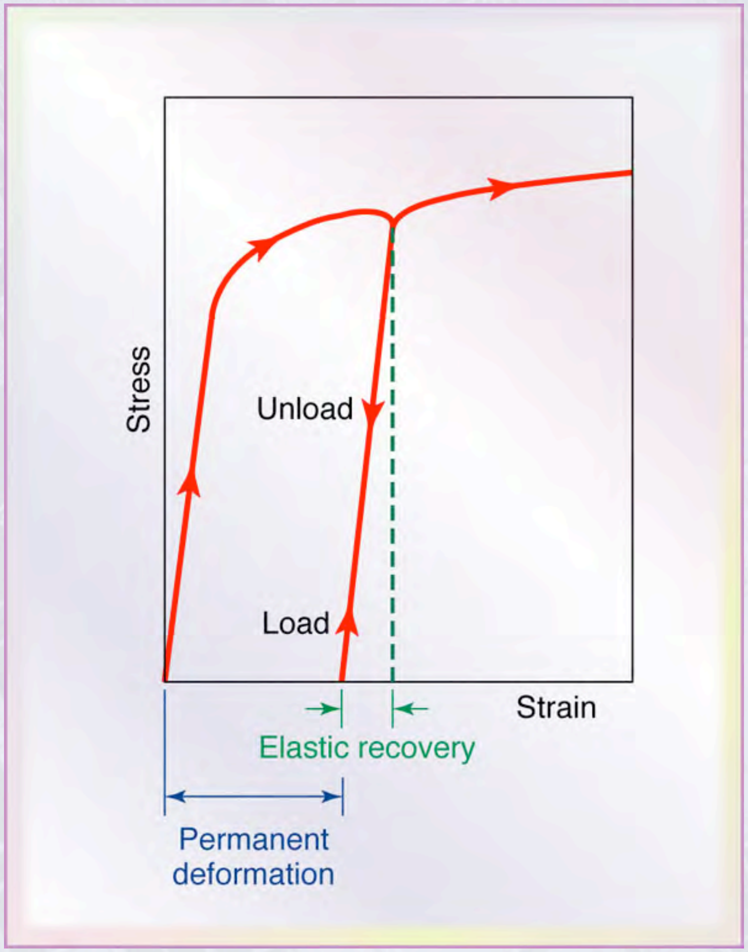

Figure 2.3 Schematic illustration of the loading and the unloading of a tensile-test specimen. Note that, during unloading, the curve follows a path parallel to the original elastic slope.

Elongation vs. Tensile-reduction

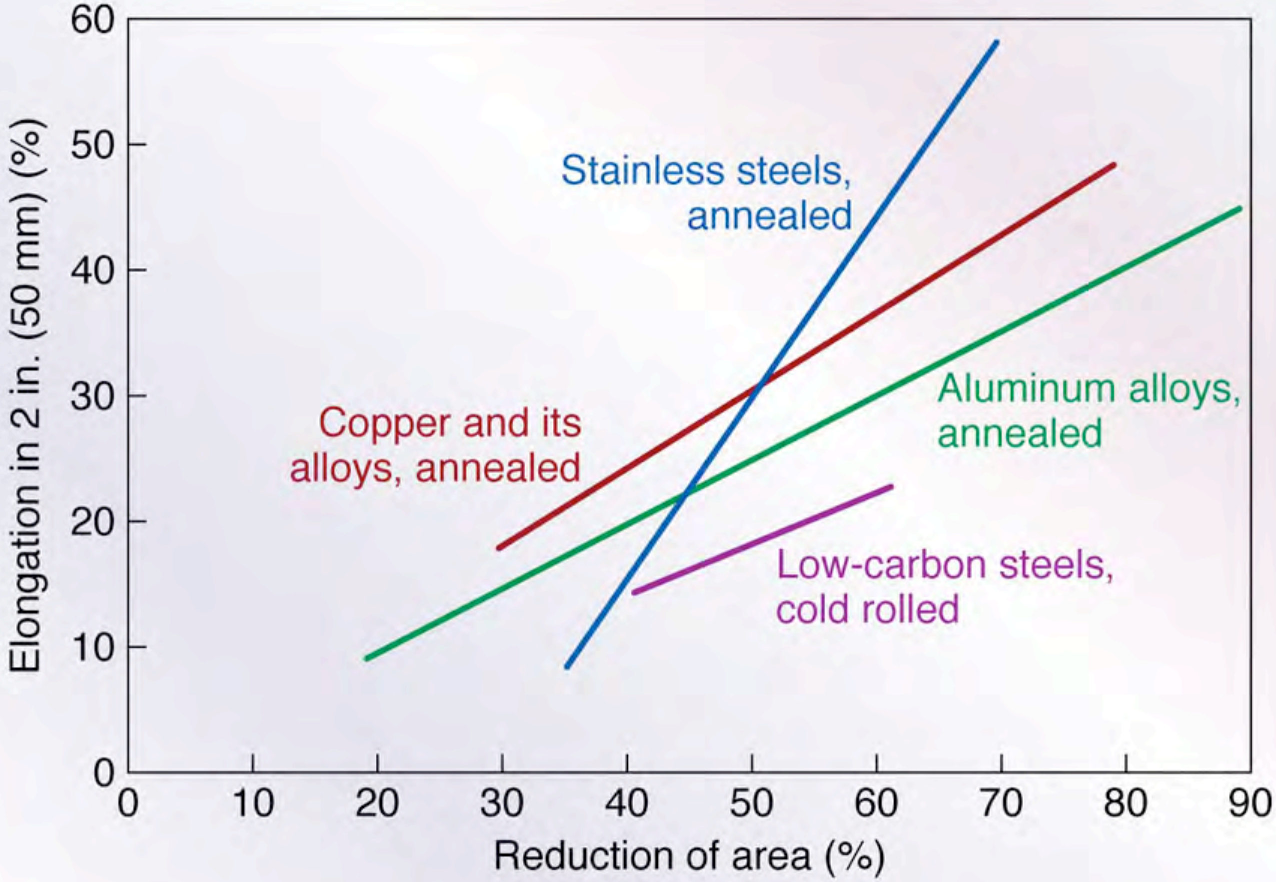

Figure 2.4 Approximate relationship between elongation and tensile reduction of area for various groups of metals

Tension and Stress Curves

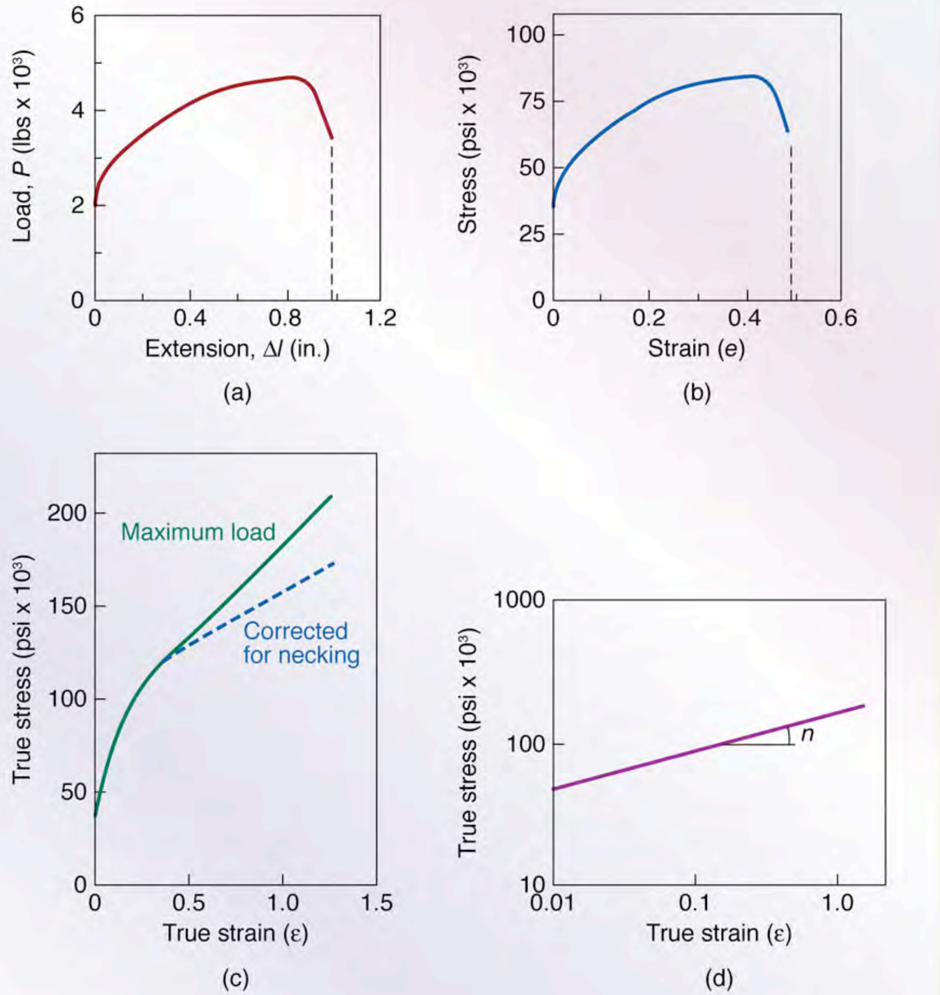

Figure 2.5 (a) Load elongation curve in tension testing of a stainless steel specimen. (b) Engineering stress-engineering strain curve, drawn from the data in Fig. 2.5a. (c) True stress-true strain curve, drawn from the data in Fig. 2.5b. Note that this curve has a positive slope, indicating that the material is becoming stringer as it is strained. (d) True stress-true strain curve plotted on the log-log paper and based on the corrected curve in Fig. 2.5c. The correction is due to the triaxial state of stress tat exists in the necked region of the specimen.

Power Law Constitutive Model

TABLE 2.3

Typical Values for *K* and *n* at Room Temperature

	K (MPa)	*n*
Aluminum		
1100 –O	180	0.20
2024 –T4	690	0.16
6061 –O	205	0.20
6061 –T6	410	0.05
7075 –O	400	0.17
Brass		
70–30, annealed	900	0.49
85–15, cold-rolled	580	0.34
Cobalt-based alloy, heat-treated	2070	0.50
Copper, annealed	315	0.54
Steel		
Low-C annealed	530	0.26
4135 annealed	1015	0.17
4135 cold-rolled	1100	0.14
4340 annealed	640	0.15
304 stainless, annealed	1275	0.45
410 stainless, annealed	960	0.10

$$\sigma = K\varepsilon^n$$

where

K = strength coefficient

n = strain hardening exponent

Manufacturing, Engineering & Technology, Fifth Edition, by Serope Kalpakjian and Steven R. Schmid.
ISBN 0-13-148965-8.

True Stress-strain Curves

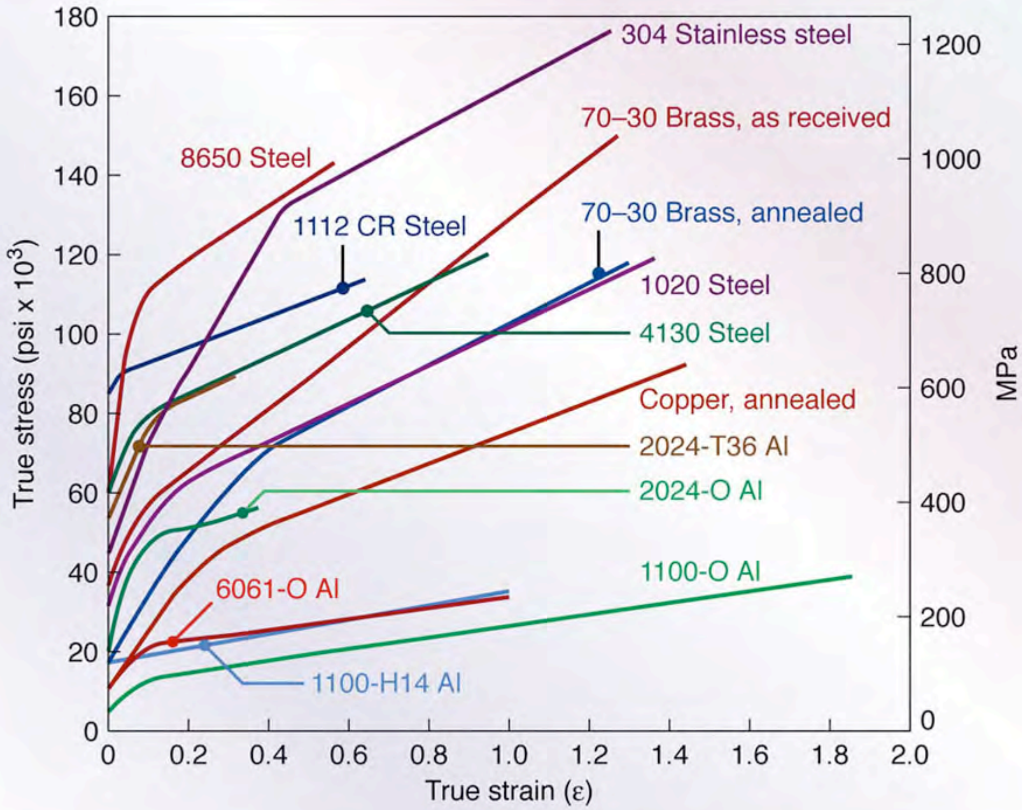

Figure 2.6 True stress-strain curves in tension at room temperature for various metals. The curves start at a finite level of stress: The elastic regions have too steep a slope to be shown in this figure, and thus each curve starts at the yield stress, Y, of the material

Manufacturing, Engineering & Technology, Fifth Edition, by Serope Kalpakjian and Steven R. Schmid.
ISBN 0-13-148965-8.

Temperature Effects on Stress-strain Curves

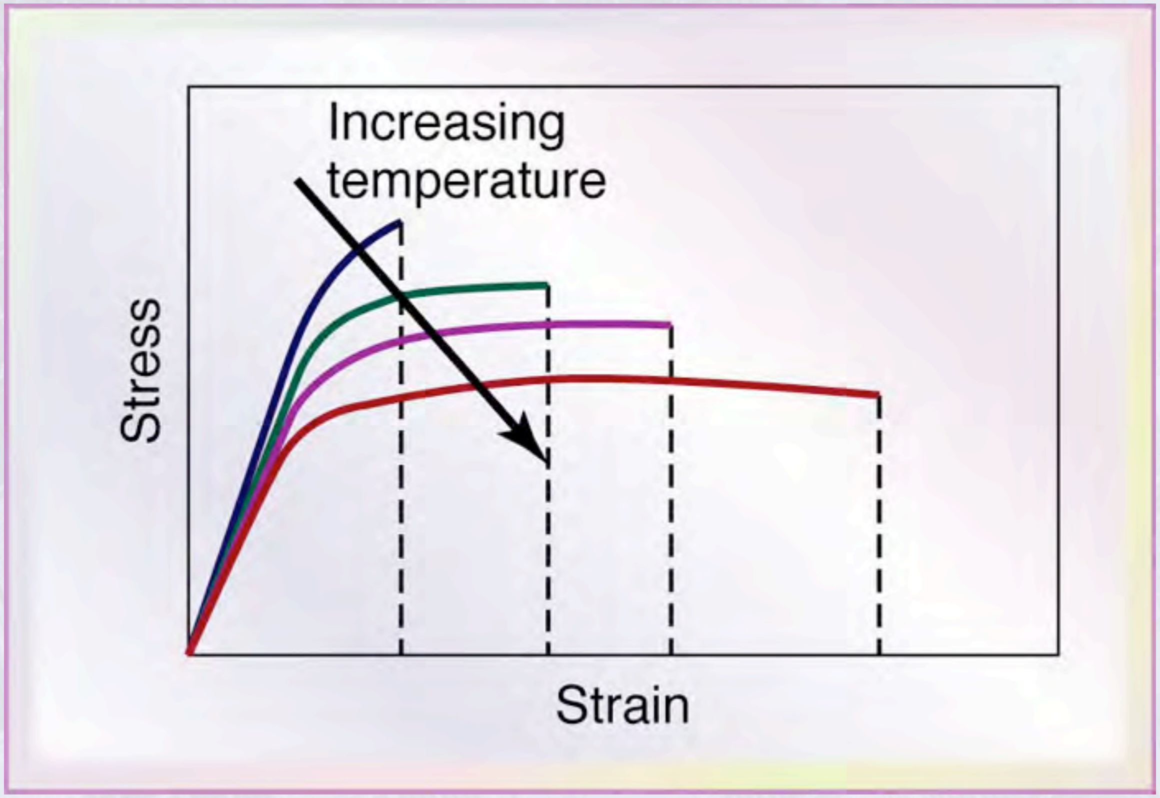

Figure 2.7 Typical effects of temperature on stress-strain curves. Note that temperature affects the modulus of elasticity, the yield stress, the ultimate tensile strength, and the toughness (area under the curve) of materials.

Manufacturing, Engineering & Technology, Fifth Edition, by Serope Kalpakjian and Steven R. Schmid.
ISBN 0-13-148965-8.

Strain and Deformation Rate in Manufacturing

TABLE 2.4

Typical Ranges of Strain and Deformation Rate in Manufacturing Processes

Process	True strain	Deformation rate (m/s)
Cold working		
Forging, rolling	0.1 –0.5	0.1 –100
Wire and tube drawing	0.05 –0.5	0.1 –100
Explosive forming	0.05–0.2	10 –100
Hot working and warm working		
Forging, rolling	0.1 –0.5	0.1 –30
Extrusion	2 –5	0.1 –1
Machining	1–10	0.1 –100
Sheet-metal forming	0.1–0.5	0.05 –2
Superplastic forming	0.2–3	10^{-4}–10^{-2}

Effect of Strain Rate on Tensile Strength of Al

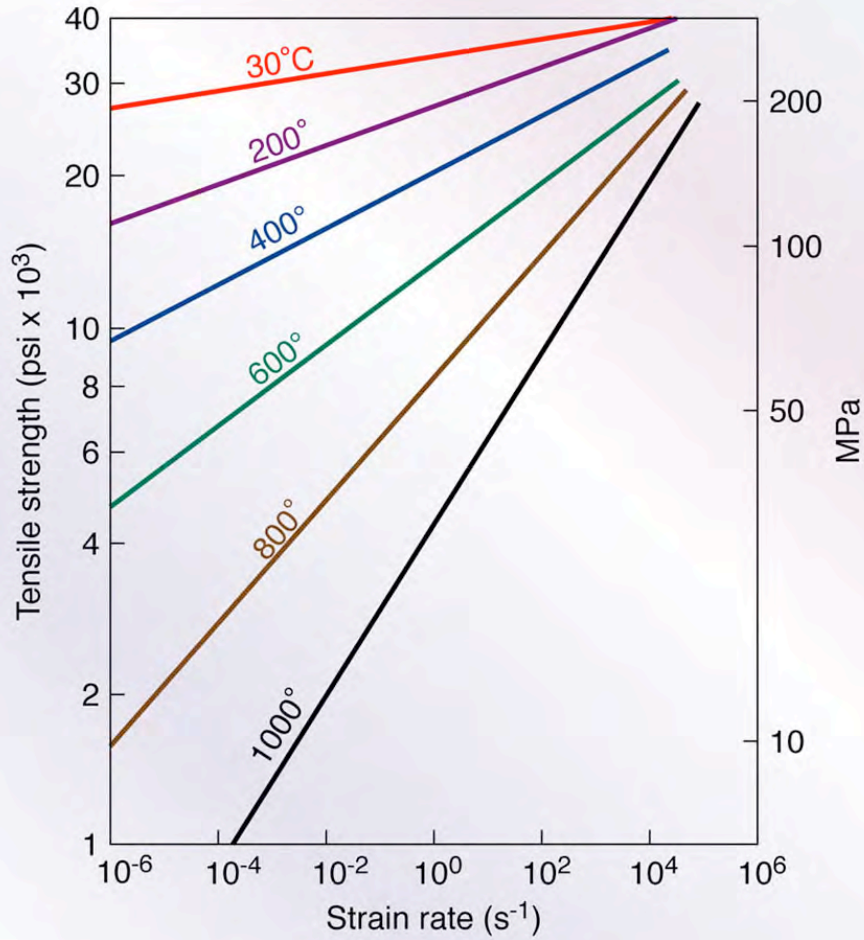

Figure 2.8 The effect of strain rate on the ultimate tensile strength for aluminum. Note that, as the temperature increases, the slopes of the curves increase; thus, strength becomes more and more sensitive to strain rate as temperature increases. *Source:* After J.H. Holloman

Manufacturing, Engineering & Technology, Fifth Edition, by Serope Kalpakjian and Steven R. Schmid.
ISBN 0-13-148965-8.

Disk Test

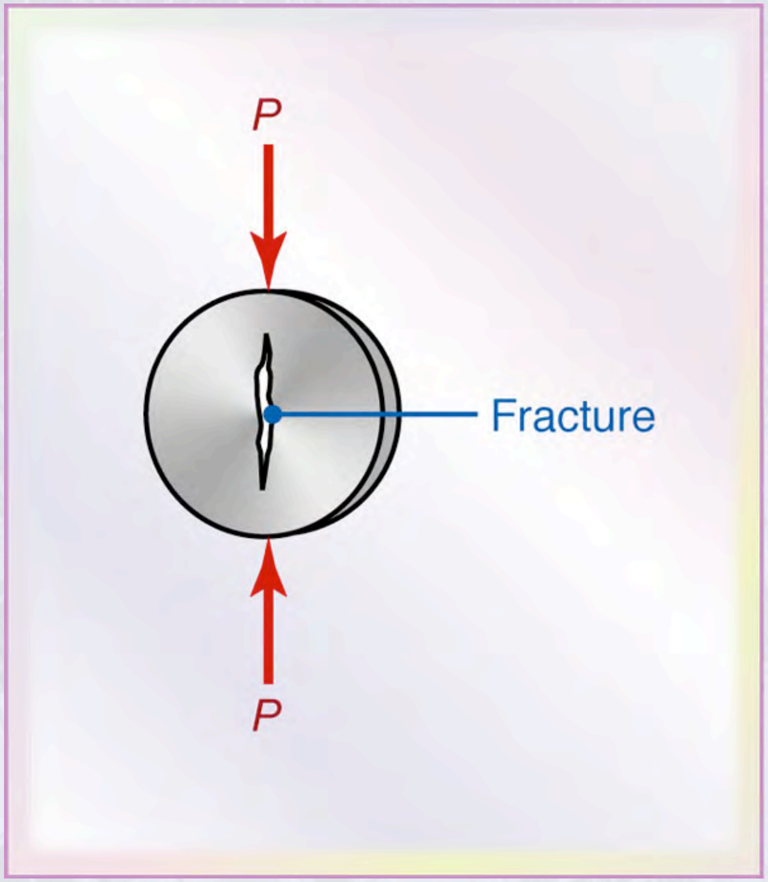

Figure 2.9 Disk test on a brittle material, showing the direction of loading and the fracture path.

$$\text{Tensile stress, } \sigma = \frac{2P}{\pi d t}$$

where

P = load at fracture

d = diameter of disk

t = thickness of disk

Manufacturing, Engineering & Technology, Fifth Edition, by Serope Kalpakjian and Steven R. Schmid.
ISBN 0-13-148965-8.

Torsion-Test Specimen

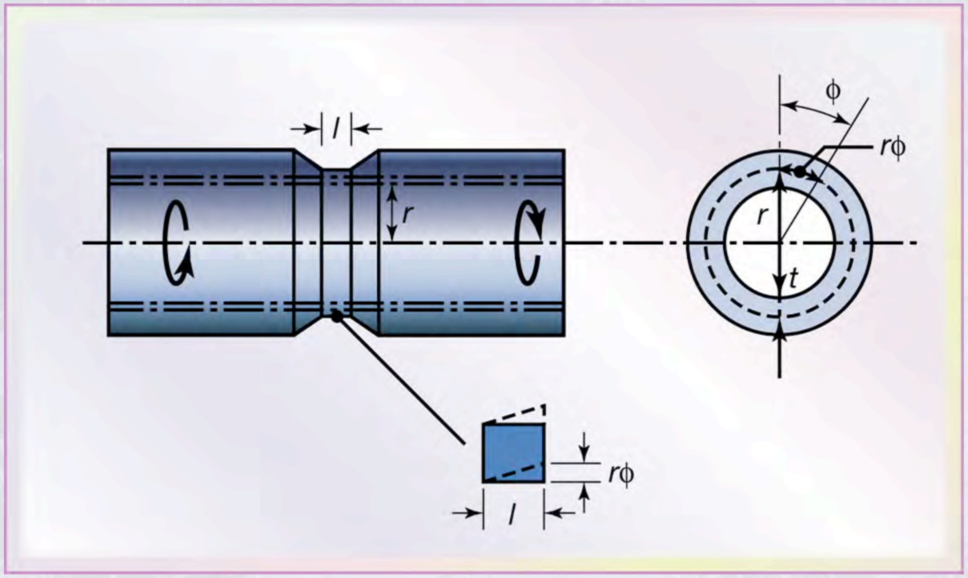

Figure 2.10 A typical torsion-test specimen; it is mounted between the two heads of a testing machine and twisted. Note the shear deformation of an element in the reduced section of the specimen.

$$\text{Shear stress, } \tau = \frac{T}{2\pi r^2 t}$$

$$\text{Shear strain, } \gamma = \frac{r\phi}{l}$$

where

T = torque

r = average tube radius

t = thickness of tube at narrow section

l = length of tube subjected to torsion

ϕ = angle of twist

Bend-test Methods

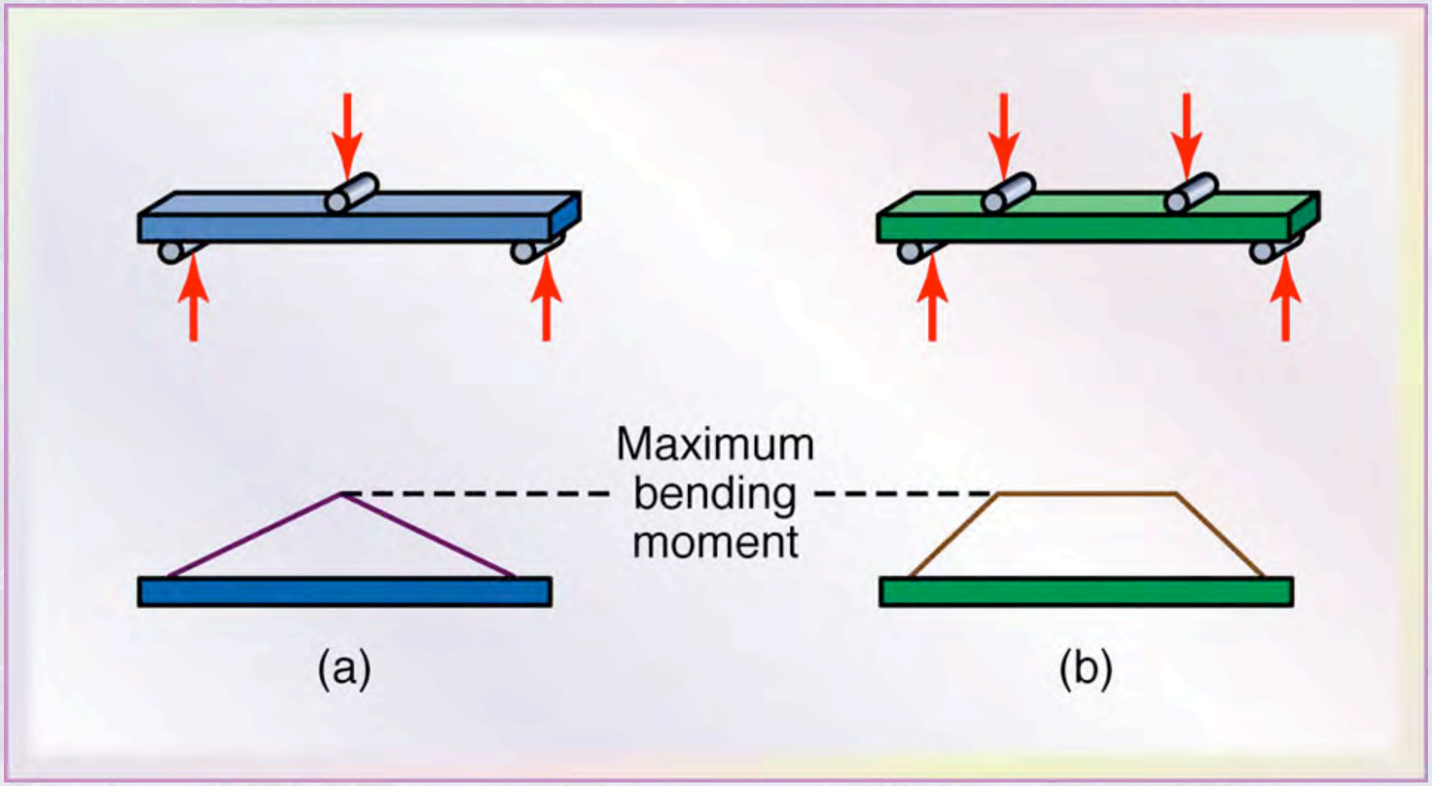

Figure 2.11 Two bend-test methods for brittle materials: (a) three-point bending; (b) four-point bending. The areas on the beams represent the bending-movement diagrams, described in texts on mechanics of solids. Note the region of constant maximum bending movement in (b); by contrast, the maximum bending moment occurs only at the center of the specimen in (a).

Manufacturing, Engineering & Technology, Fifth Edition, by Serope Kalpakjian and Steven R. Schmid.
ISBN 0-13-148965-8.

Hardness-testing Methods and Formulas

Test	Indenter	Shape of indentation: Side view	Shape of indentation: Top view	Load, P	Hardness number
Brinell	10-mm steel or tungsten carbide ball	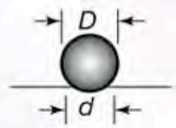 D, d	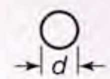 d	500 kg 1500 kg 3000 kg	$HB = \frac{2P}{(\pi D)(D - \sqrt{D^2 - d^2})}$
Vickers	Diamond pyramid	 136°	 L	1–120 kg	$HV = \frac{1.854P}{L^2}$
Knoop	Diamond pyramid	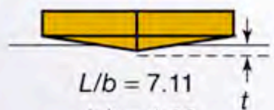 $L/b = 7.11$ $b/t = 4.00$ t	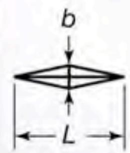 b, L	25 g–5 kg	$HK = \frac{14.2P}{L^2}$
Rockwell					
A C D	Diamond cone	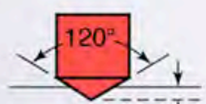 120° t = mm		60 kg 150 kg 100 kg	HRA HRC HRD } $= 100 - 500t$
B F G	$\frac{1}{16}$- in. diameter steel ball	 t = mm		100 kg 60 kg 150 kg	HRB HRF HRG } $= 130 - 500t$
E	$\frac{1}{8}$- in. diameter steel ball			100 kg	HRE

Figure 2.12 General characteristics of hardness-testing methods and formulas for calculating hardness.

Manufacturing, Engineering & Technology, Fifth Edition, by Serope Kalpakjian and Steven R. Schmid.
ISBN 0-13-148965-8.

Indentation Geometry for Brinnel Testing

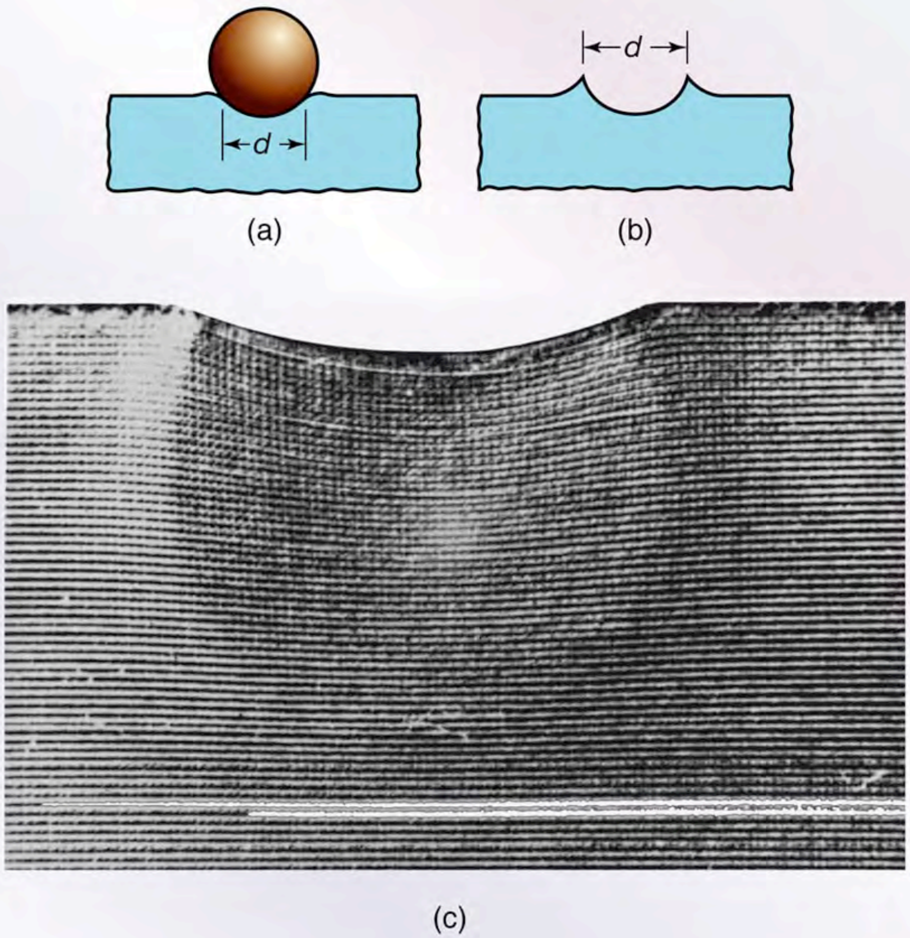

Figure 2.13 Indentation geometry in Brinell hardness testing: (a) annealed metal; (b) work-hardened metal; (c) deformation of mild steel under a spherical indenter. Note that the depth of the permanently deformed zone is about one order of magnitude larger that the depth of indentation. For a hardness test to be valid, this zone should be developed fully in the material. *Source:* Courtesy of M.C. Shaw and C.T. Yang

Manufacturing, Engineering & Technology, Fifth Edition, by Serope Kalpakjian and Steven R. Schmid.
ISBN 0-13-148965-8.

Hardness Scale Conversions

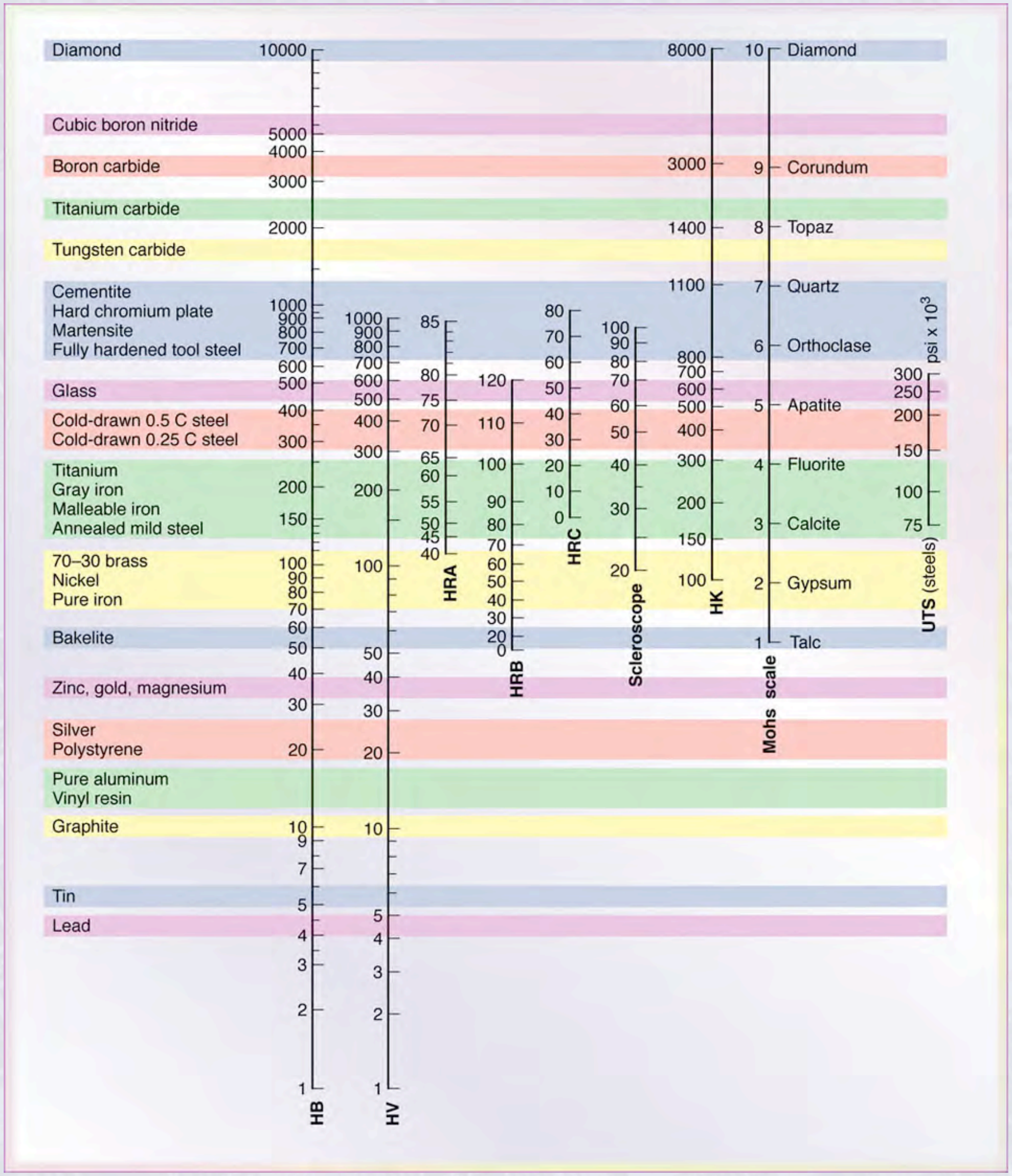

Figure 2.14 Chart for converting various hardness scales. Note the limited range of most scales. Because of the many factors involved, these conversions are approximate.

ISBN 0-13-148965-8.

S-N Curves

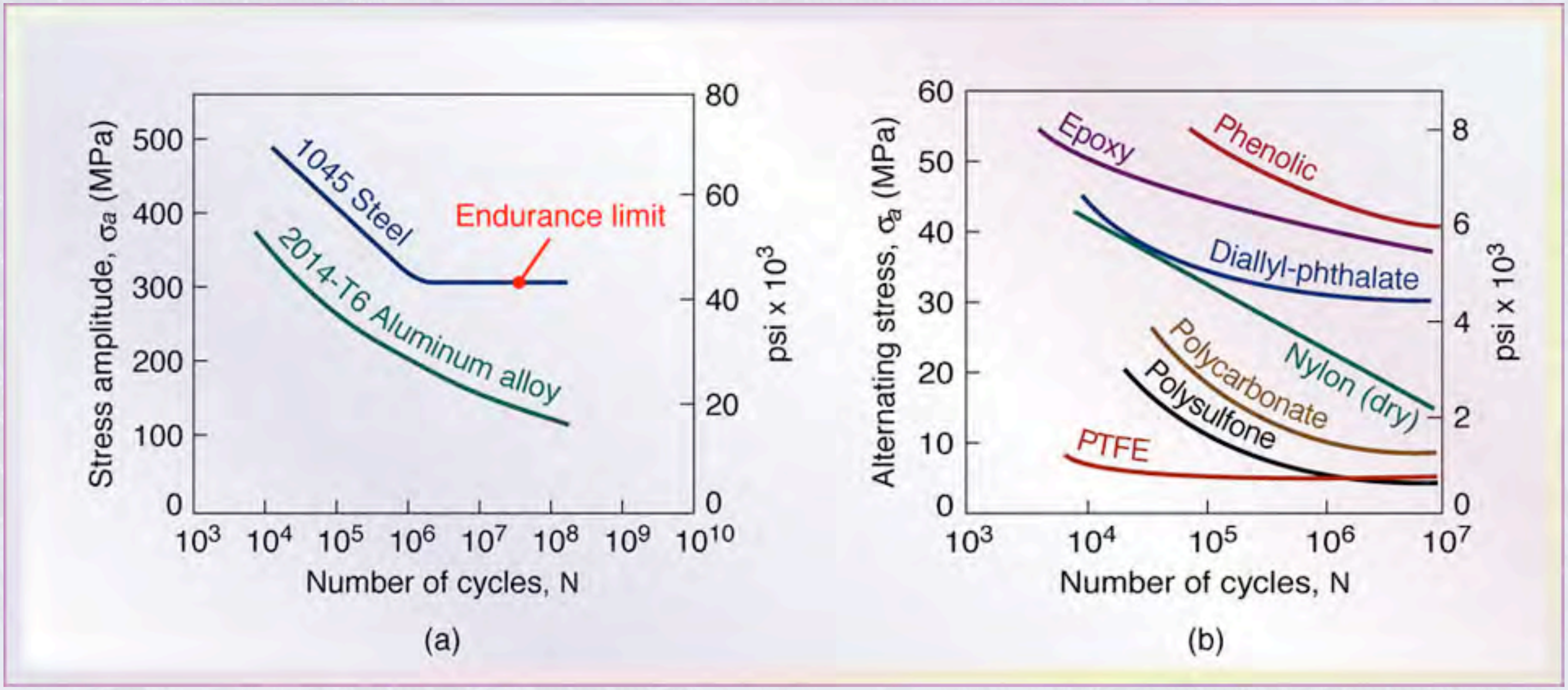

Figure 2.15 (a) Typical S-N curves for two metals. Note that, unlike steel, aluminum does not have an endurance limit. (b) S-N curves for common polymers

Manufacturing, Engineering & Technology, Fifth Edition, by Serope Kalpakjian and Steven R. Schmid.
ISBN 0-13-148965-8.

Endurance Limit vs. Tensile Strength

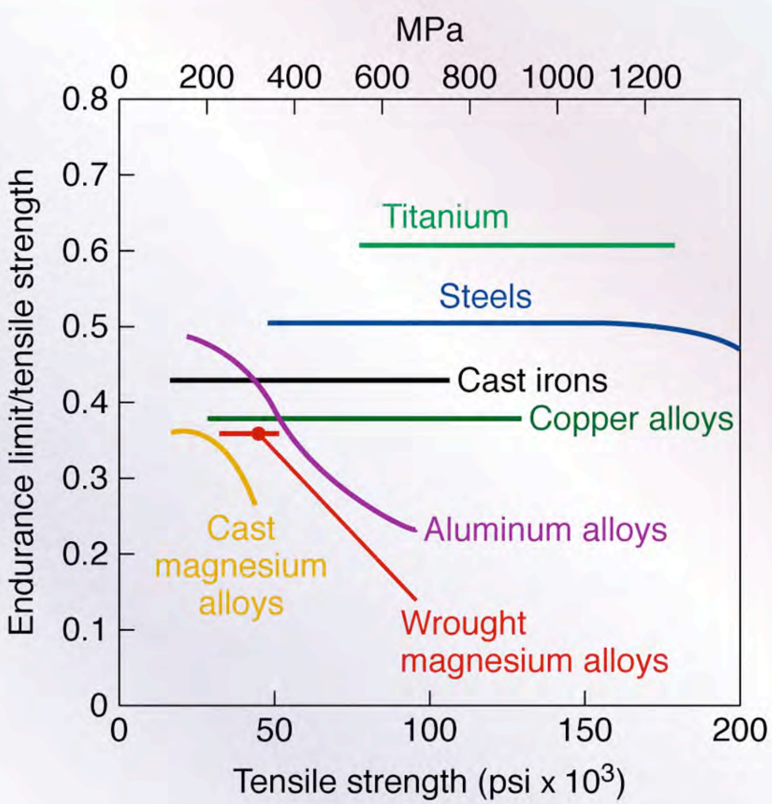

Figure 2.16 Ratio of endurance limit to tensile strength for various metals, as a function of tensile strength. Because aluminum does not have an endurance limit, the correlations for aluminum are based on a specific number of cycles, as is seen in Fig. 2.15.

Manufacturing, Engineering & Technology, Fifth Edition, by Serope Kalpakjian and Steven R. Schmid.
ISBN 0-13-148965-8.

Creep Curve

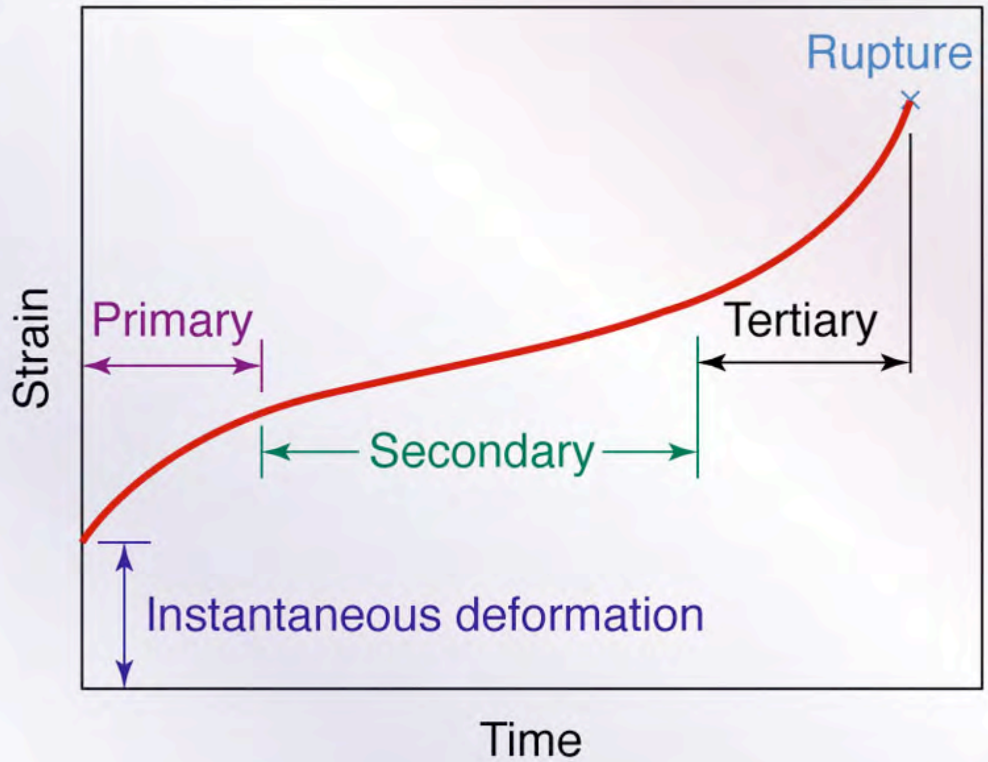

Figure 2.17 Schematic illustration of a typical creep curve. The linear segment of the curve (secondary) is used in designing components for a specific creep life.

Impact Test Specimens

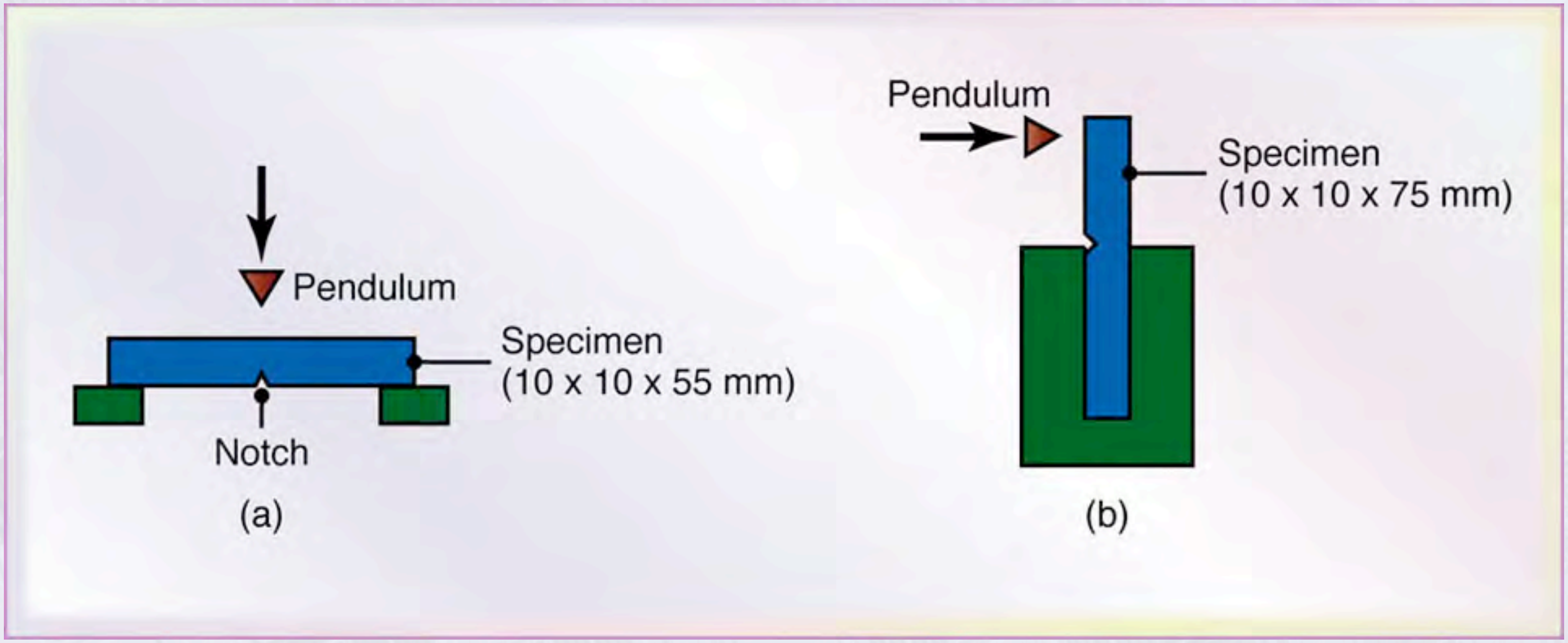

Figure 2.18 Impact test specimens: (a) Charpy; (b) Izod.

Material Failures

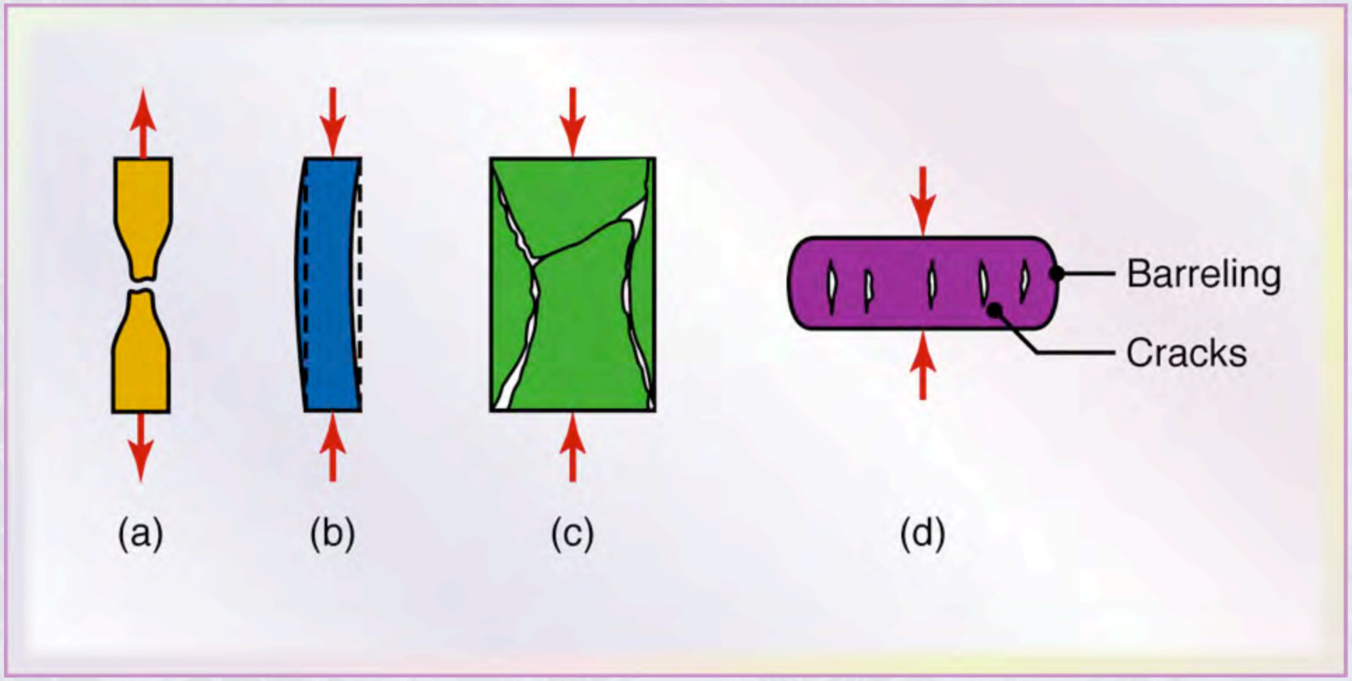

Figure 2.19 Schematic illustrations of types of failures in materials: (a) necking and fracture of ductile materials; (b) buckling of ductile materials under a compressive load; (c) fracture of brittle materials in compression; (d) cracking on the barreled surface of ductile materials in compression

Manufacturing, Engineering & Technology, Fifth Edition, by Serope Kalpakjian and Steven R. Schmid.
ISBN 0-13-148965-8.

Fracture Types in Tension

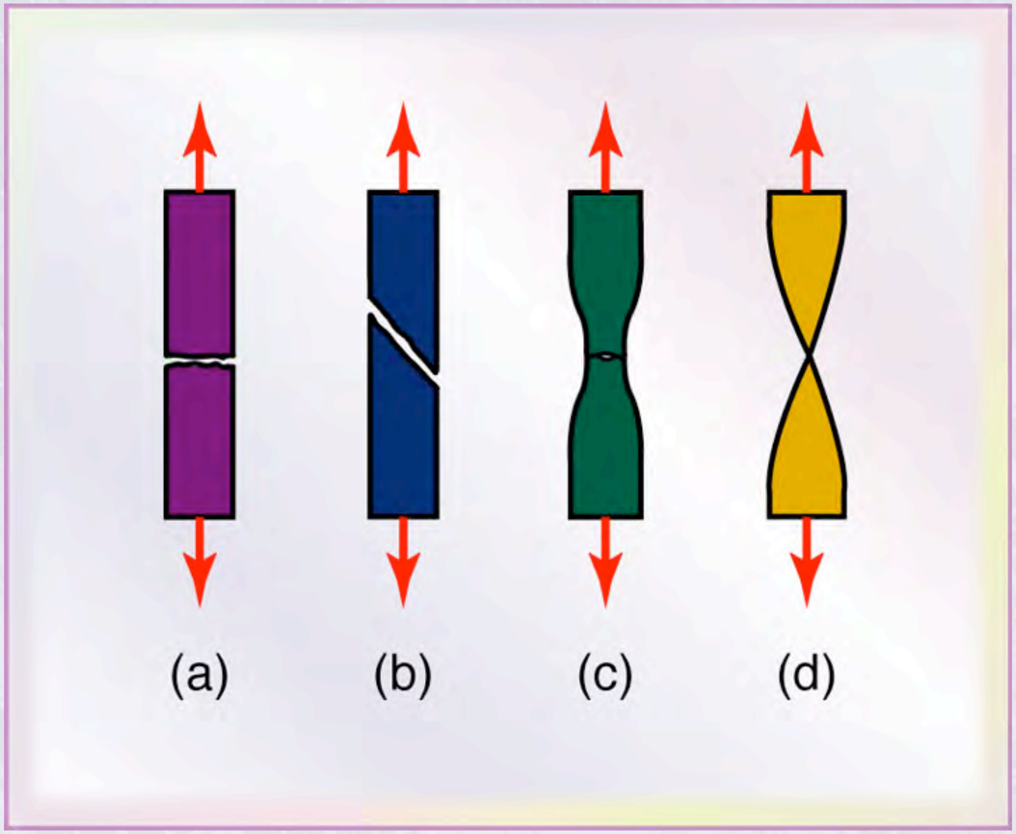

Figure 2.20 Schematic illustration of the types of fracture in tension: (a) brittle fracture in polycrystalline metals; (b) shear fracture in ductile single crystals – see also Fig 1.6a; (c) ductile cup-and-cone fracture in polycrystalline metals; (d) complete ductile fracture in polycrystalline metals, with 100% reduction of area.

Ductile Fracture in Low-carbon Steel

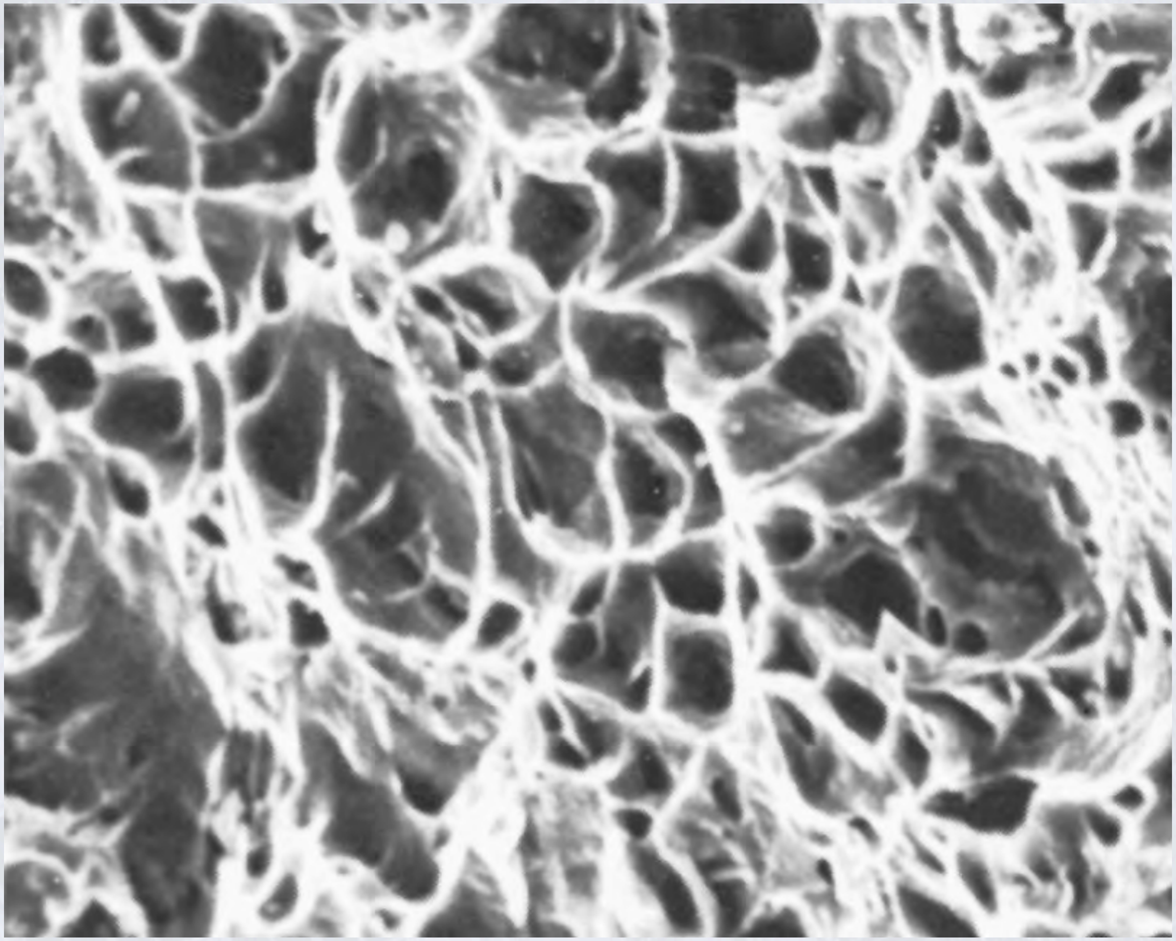

Figure 2.21 Surface of ductile fracture in low-carbon steel, showing dimples. Fracture usually is initiated at impurities, inclusions, or preexisting voids (microporosity) in the metal. *Source*: Courtesy of K. H. Habig and D. Klaffke

Manufacturing, Engineering & Technology, Fifth Edition, by Serope Kalpakjian and Steven R. Schmid.
ISBN 0-13-148965-8.

Progression of a Fracture

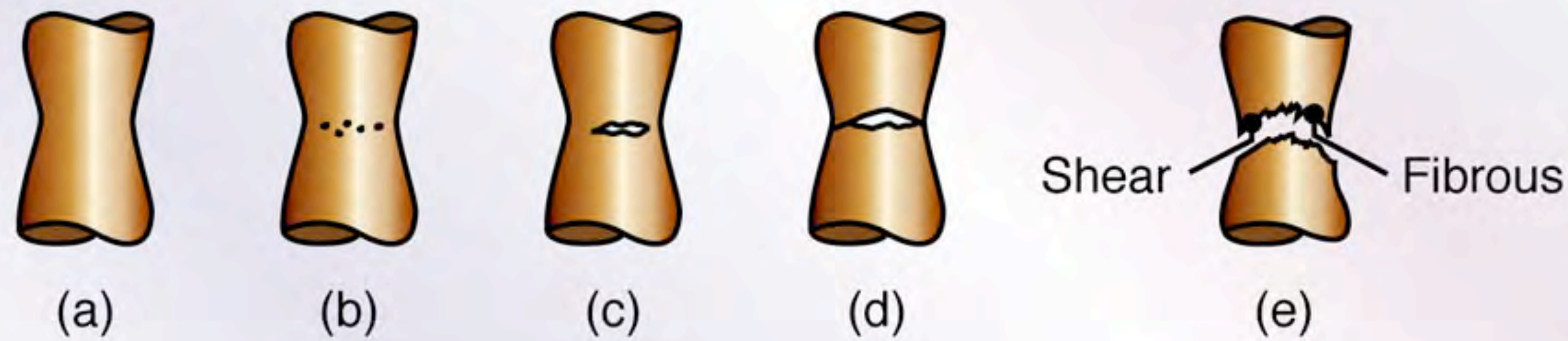

Figure 2.22 Sequence of events in the necking and fracture of a tensile-test specimen: (a) early stage of necking; (b) small voids begin to form within the necked region; (c) voids coalesce, producing an internal crack; (d) the rest of the cross-section begins to fail at the periphery, by shearing; (e) the final fracture surfaces, known as cup- (top fracture surface) and cone- (bottom surface) fracture.

Manufacturing, Engineering & Technology, Fifth Edition, by Serope Kalpakjian and Steven R. Schmid.
ISBN 0-13-148965-8.

Deformation of Inclusions and Their Effect on Void Formation

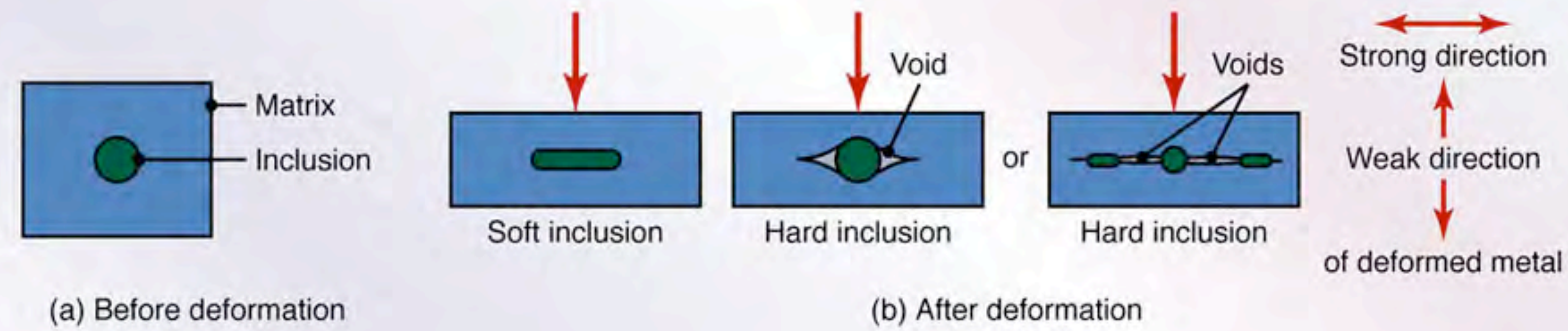

Figure 2.23 Schematic illustration of the deformation of soft and hard inclusions and of their effect on void formation in plastic deformation. Note that, because they do not conform to the overall deformation of the ductile matrix, hard inclusions can cause internal voids.

Manufacturing, Engineering & Technology, Fifth Edition, by Serope Kalpakjian and Steven R. Schmid.
ISBN 0-13-148965-8.

Temperature Transition in Metals

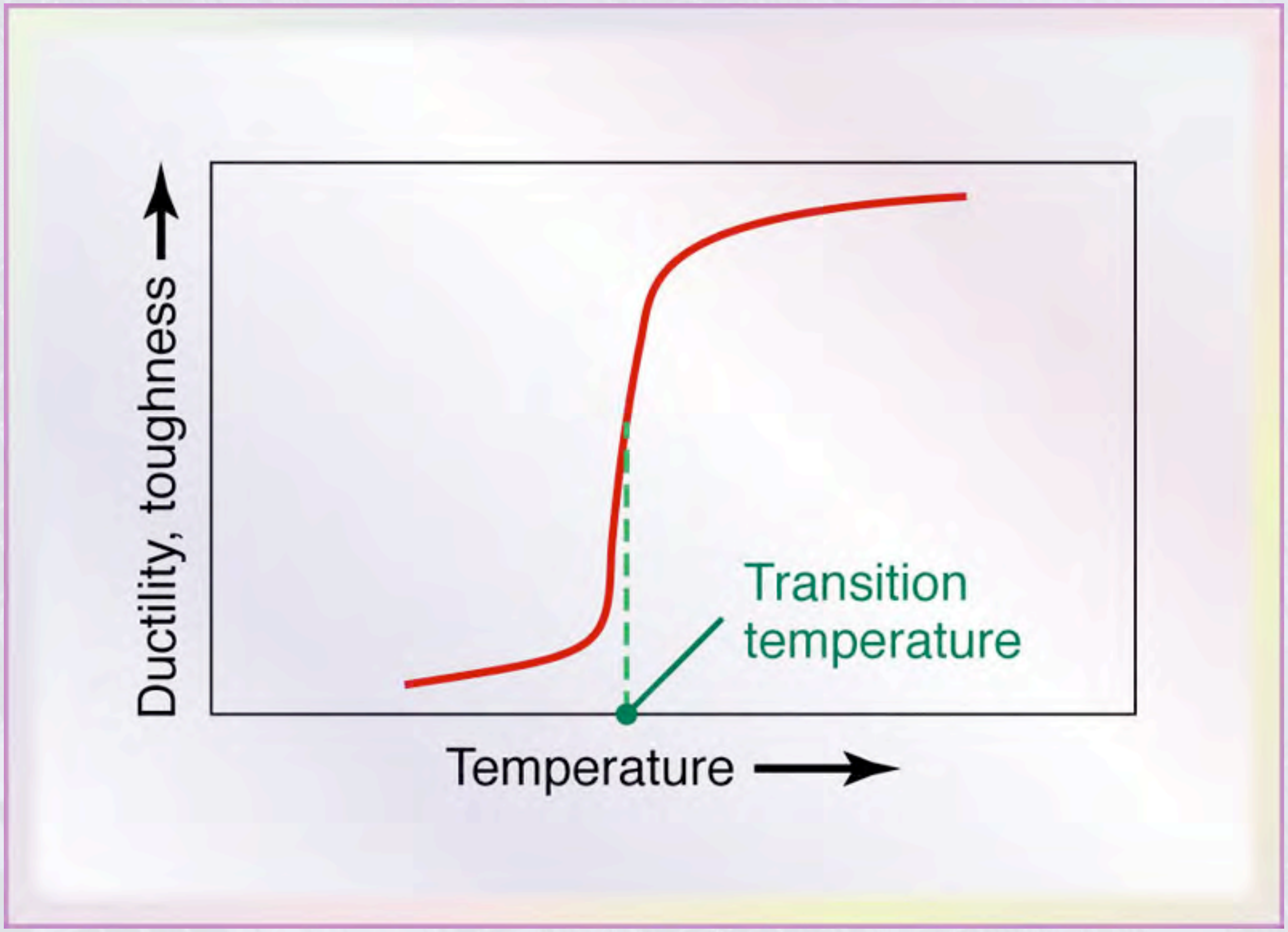

Figure 2.24 Schematic illustration of transition temperature in metals.

Fracture Surface of Steel

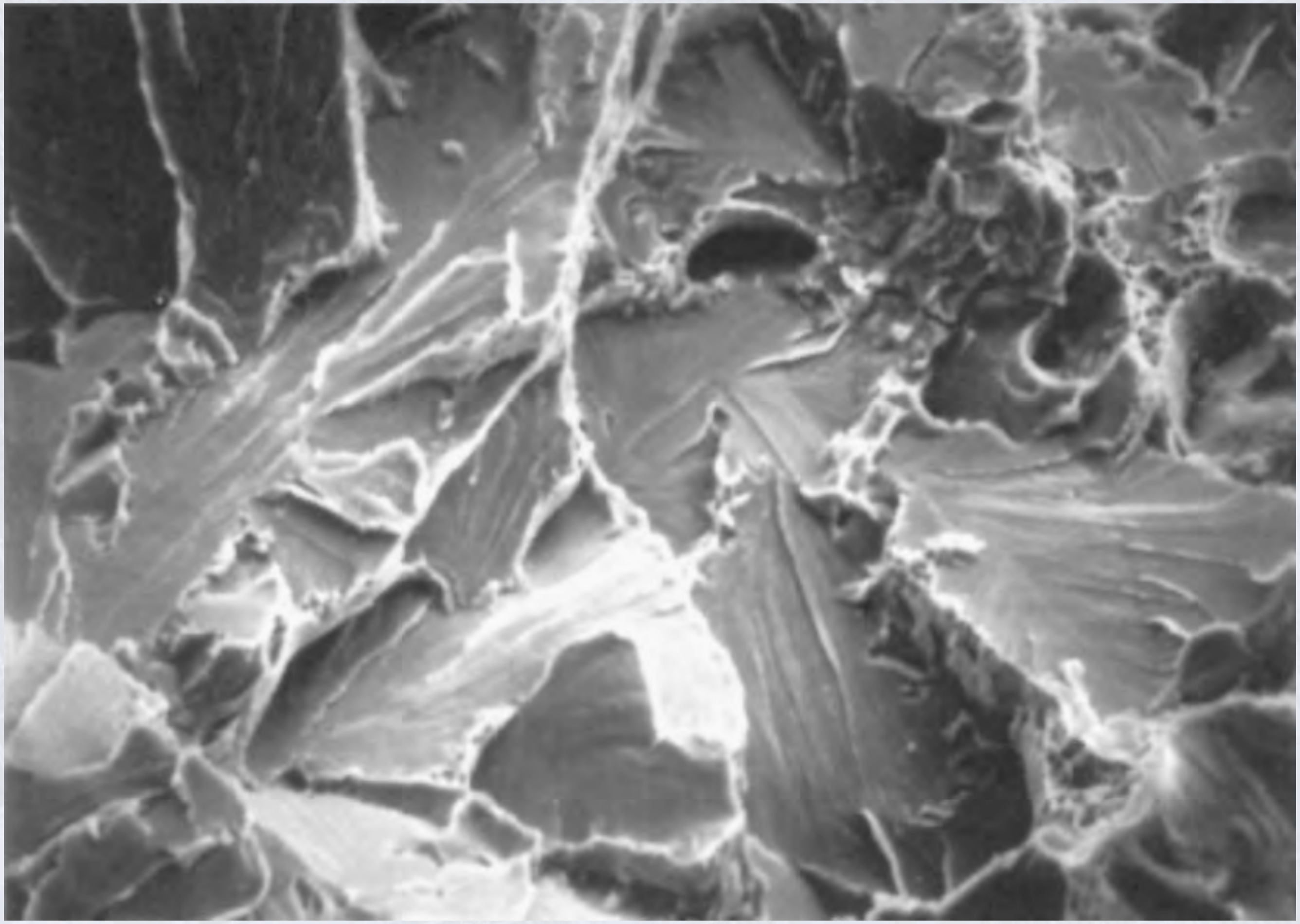

Figure 2.25 Fracture surface of steel that has failed in a brittle manner. The fracture path is transgranular (through the grains). Magnification: 200x. *Source:* Courtesy of B. J. Schulze and S.L. Meinley and Packer Engineering Associates, Inc.

Intergranular Fracture

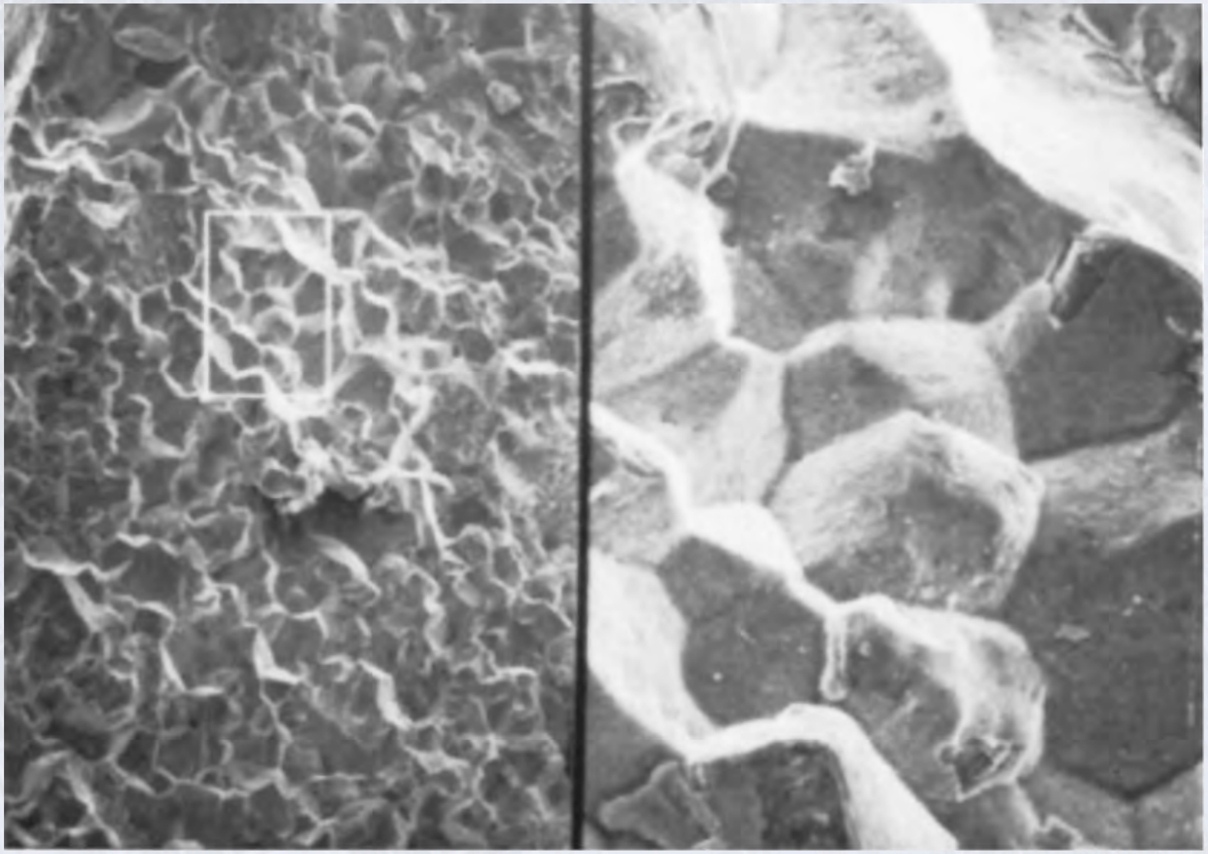

Figure 2.26 Intergranular fracture, at two different magnifications. Grains and grain boundaries are clearly visible in this micrograph. The fracture path is along the grain boundaries. Magnification: left, 100x; right, 500x. *Source*: Courtesy of B.J. Schulze and S.L. Meiley and Packer Engineering Associates, Inc.

Fatigue-Fracture Surface

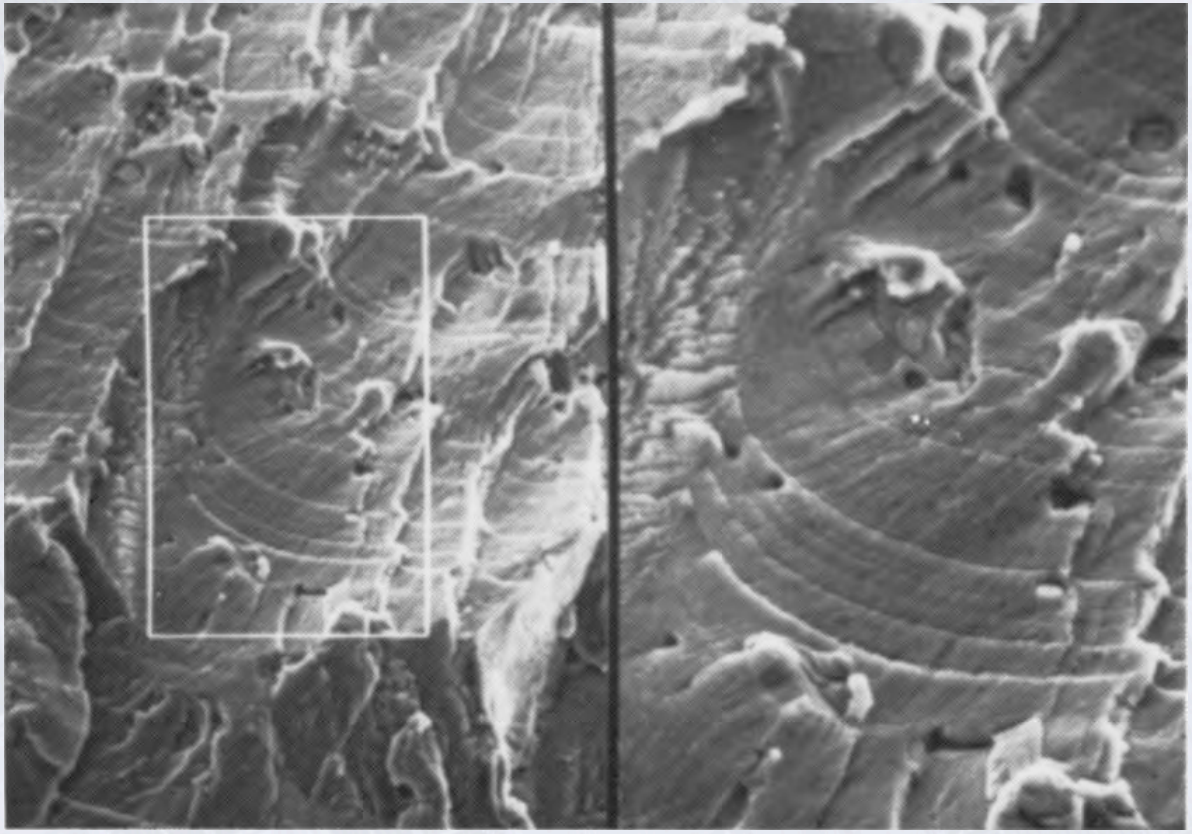

Figure 2.28 Typical fatigue-fracture surface on metals, showing beach marks. Magnification: left, 500x; right, 1000x. *Source*: Courtesy of B.J. Schulze and S.L. Meiley and Packer Engineering Associates, Inc.

Reduction in Fatigue Strength vs. Ultimate Tensile Strength

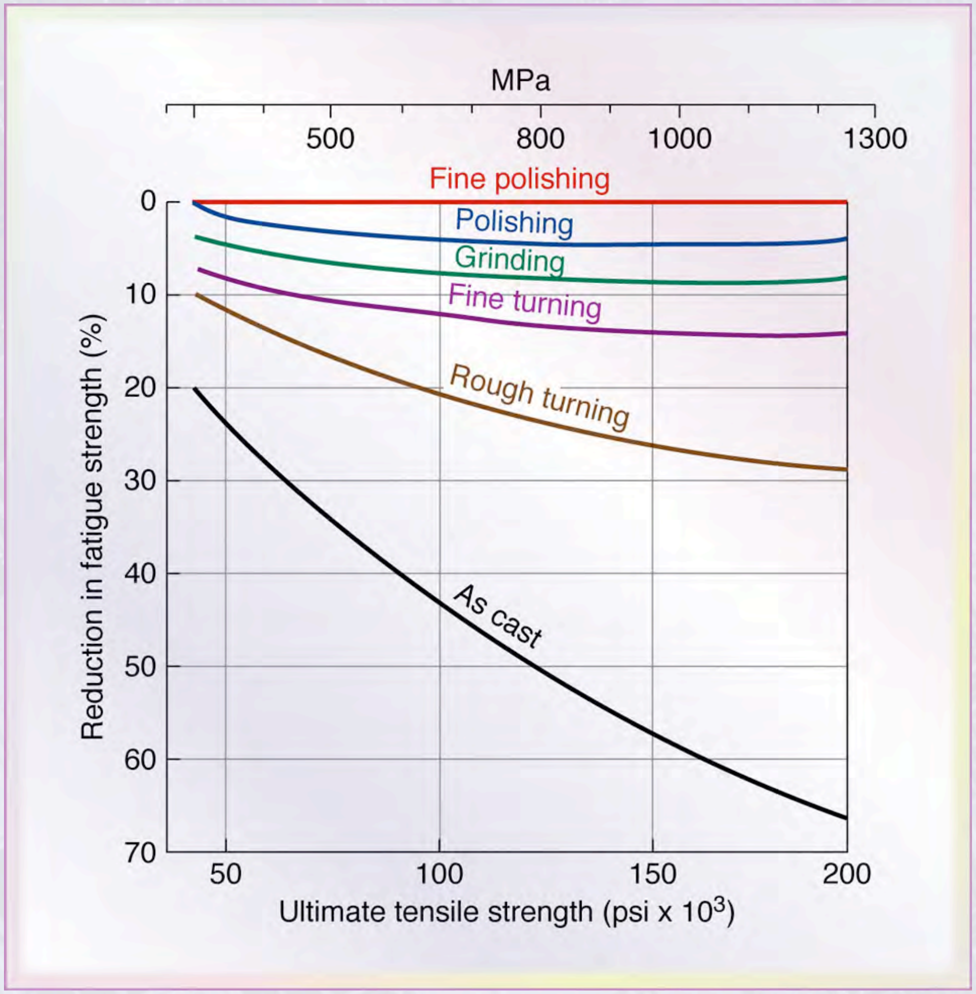

Figure 2.28 Reductions in fatigue strength of cast steels subjected to various surface-finishing operations. Note that the reduction becomes greater as the surface roughness and the strength of steel increase. *Source:* Courtesy of M. R. Mitchell

Residual Stresses in Bending a Beam

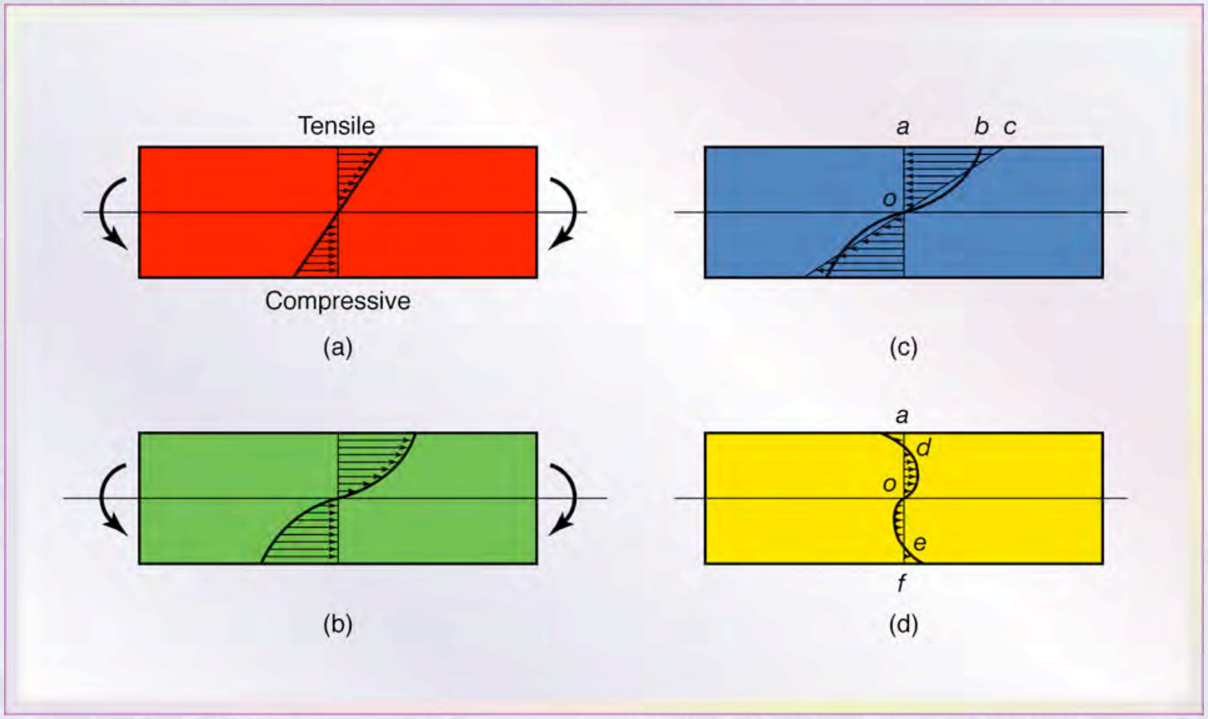

Figure 2.29 Residual stresses developed in bending a beam having a rectangular cross-section. Note that the horizontal forces and moments caused by residual stresses in the beam must be balanced internally. Because of nonuniform deformation and especially during cold-metalworking operations, most parts develop residual stresses.

Manufacturing, Engineering & Technology, Fifth Edition, by Serope Kalpakjian and Steven R. Schmid.
ISBN 0-13-148965-8.

Distortion with Residual Stresses

Figure 2.30 Distortion of parts, with residual stresses, after cutting or slitting: (a) flat sheet or plate; (b) solid round rod; (c) thin-walled tubing or pipe.